

# Finite Element Analysis and Validation of SIF and J-Integral of a Semi-elliptical crack with Analytical Method

Yugal Kishor Sahu\*, S. K. Moulick\*\*

## Abstract

Crack in any machine component leads to a catastrophic phenomenon by sudden and total collapse. So, it is required to predict the behavior of a machine component under subjection of load both in static state or dynamic state. For proper prediction about failure of any object it is required to perfectly measure Stress Intensity Factor and J-Integral of a crack induced in that machine component under the action of static or dynamic loading. It is not possible to calculate SIF and J-Integral for all crack configurations analytically. So, numerical method is very efficient to calculate the SIF and J-Integral for any crack configuration. Here in this paper a validation has been done in calculating SIF and J-Integral of a semi-elliptical crack in an rectangular block using analytical formulas and using a FEA software named ANSYS Workbench to calculate numerically.

**Keywords:** Semi-elliptical Crack, Stress Intensity Factor (SIF), J-Integral, ANSYS

such as linear kinetic energy combining two variables to one, linear momentum combining two variables to one, Reynolds Number in fluid mechanics combining four independent variables to one, and Sommerfield Number in journal bearing combining five variables into one.

Now we know that the stress field at a general point H near the crack tip for isotropic and linear elastic material in the flat plate for Mode I case is

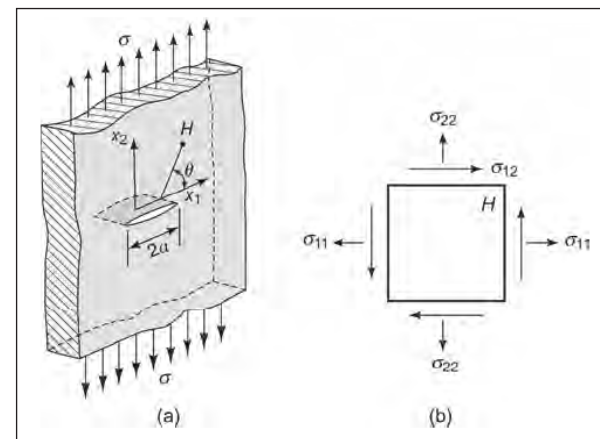


**Fig 1:** (a) Infinite Plate with A Crack of Length 2a Subjected to a Far Field Stress  $\sigma$ , and (b) Definition of Stress Components at Point H

$$\sigma_{11} = \frac{\sigma(\pi a)^{1/2}}{(2\pi r)^{1/2}} \cos \frac{\theta}{2} \left[ 1 - \sin \frac{\theta}{2} \sin \frac{3\theta}{2} \right] \quad (1a)$$

$$\sigma_{22} = \frac{\sigma(\pi a)^{1/2}}{(2\pi r)^{1/2}} \cos \frac{\theta}{2} \left[ 1 + \sin \frac{\theta}{2} \sin \frac{3\theta}{2} \right] \quad (1b)$$

$$\sigma_{12} = \frac{\sigma(\pi a)^{1/2}}{(2\pi r)^{1/2}} \sin \frac{\theta}{2} \cos \frac{\theta}{2} \cos \frac{3\theta}{2} \quad (1c)$$

$$\sigma_{11} = \frac{K_I}{(2\pi r)^{1/2}} \cos \frac{\theta}{2} \left[ 1 - \sin \frac{\theta}{2} \sin \frac{3\theta}{2} \right] \quad (1a)$$

## INTRODUCTION

In the engineering field, a problem with two variables is much more difficult to solve than a problem of one variable. A question may be raised here—can two independent variables be combined to form a new independent variable? If the answer is yes, the solution to the problem is likely to become much simpler. In the case of a wave propagation, solution even along one dimension becomes complex because two variables, space (x) and time (t), are involved. In such wave problems, we usually combine two variables to form a new variable, (x – ct), where c is the velocity of the sound. There are many other similar cases

\* Research scholar Chhattisgarh Swami Vivekananda Technical University, Bilai, Chhattisgarh, India.  
Email: sahyugal@gmail.com

\*\* Professor, B.I.T. Durg, Chhattisgarh, India. Email: sankarmoulick\_1963@yahoo.co.in

$$\sigma_{22} = \frac{K_I}{(2\pi r)^{1/2}} \cos \frac{\theta}{2} \left[ 1 + \sin \frac{\theta}{2} \sin \frac{3\theta}{2} \right] \quad (1b)$$

$$\sigma_{12} = \frac{K_I}{(2\pi r)^{1/2}} \sin \frac{\theta}{2} \cos \frac{\theta}{2} \cos \frac{3\theta}{2} \quad (1c)$$

$$u_1 = \frac{K_I}{\mu} \left( \frac{r}{2\pi} \right)^{1/2} \cos \frac{\theta}{2} \left[ 1 - 2\nu + \sin^2 \frac{\theta}{2} \right] \quad (1d)$$

$$u_2 = \frac{K_I}{\mu} \left( \frac{r}{2\pi} \right)^{1/2} \sin \frac{\theta}{2} \left[ 2 - 2\nu + \cos^2 \frac{\theta}{2} \right]. \quad (1e)$$

For a thin plate, other stress components are negligible. In case of a thick plate where  $\nu$  is the Poisson's Ratio of the material; the other two stress components ( $\sigma_{13}$ ,  $\sigma_{23}$ ) are negligible.

It is clear from these equations that each stress component is proportional to the far field stress  $\sigma$ . The crack length appears under a square root and, therefore, its influence on stress components is also prominent, but not to the extent of  $\sigma$ .

The distance ( $r$ ) between the crack tip and the point plays the most important role. It sits in the denominator under a square root sign. If  $r$  becomes very small, the stress components, especially  $\sigma_{22}$  goes up steeply, so much so that for  $r \rightarrow 0$ ,  $\sigma_{22}$  tends to be infinite. Such solutions are called singular. In this case, it is known as square root singularity. In some special cases of fracture mechanics, other kinds of singularities are encountered.

Displacement field for a plane strain near the crack tip for Mode I of Fig. 1(a) is given by

$$u_1 = \frac{\sigma(\pi a)^{1/2}}{\mu} \left( \frac{r}{2\pi} \right)^{1/2} \cos \frac{\theta}{2} \left[ 1 - 2\nu + \sin^2 \frac{\theta}{2} \right] \quad (2a)$$

$$u_2 = \frac{\sigma(\pi a)^{1/2}}{\mu} \left( \frac{r}{2\pi} \right)^{1/2} \sin \frac{\theta}{2} \left[ 2 - 2\nu + \cos^2 \frac{\theta}{2} \right] \quad (2b)$$

$$u_3 = 0 \quad (2c)$$

where  $\mu$  is the shear modulus. The above equations do not contain any singularity, because displacement is finite near the crack tip. Mathematically, displacement components are obtained from stress equations by converting stress components to strain components and then integrating the resulting expressions. During integration, the square root singularity disappears and displacement components turn out to be proportional to the square root of the distance  $r$ . However, one should note here that the Equations (2a–c)

are valid only in the close vicinity of the crack tip.

If we look carefully into Equations (1) and (2), we find that for a given geometry there are two main variables, the far field stress  $s$  and the crack length  $a$ . Furthermore, in all the equations of stress and displacement,  $\sigma$  and  $a$  coexist as  $\sigma\sqrt{a}$ . Can this product be called by a different variable? Now with several decades of research work, we find that it is advantageous to do so. This credit goes to Irwin [1], who defined the new variable, stress intensity factor, and used the symbol  $K$  after the name of his collaborator Kies [2]. He defined  $K$  as

$$K_I = \sigma (\pi a)^{1/2} \quad (3)$$

There is no reason to have  $\pi$  in the above definition. It was included in the expression because of some historical reasons. However, the stress intensity factor  $K_I$  is formally defined as

$$K_I = (2\pi r)^{1/2} \sigma_{22}(r, \theta = 0) \text{ as } r \rightarrow 0 \quad (4)$$

This definition can be checked easily by substituting Eq. (1b) in the formal definition [Eq. (4)], the resulting expression will be the same as of Eq. (3).

We realize that, for stress or displacement fields, magnitude of  $s$  or  $a$  is immaterial as long as  $\sigma(\pi a)^{1/2}$  is same. This means a small crack length in a plate with high far field stress is equivalent to a large crack length with small far field stress, provided  $K$  remains same. This combination of  $s$  and  $a$  to form a new variable is regarded as a breakthrough in the field of fracture mechanics. For Modes I–III, the stress intensity factor is written as  $K_I$ ,  $K_{II}$  and  $K_{III}$  respectively, with subscript in Roman numbers.

The stress and displacement Eqs (1) and (2) may now be written in terms of the stress intensity factor. For Mode I problems of plane strain, they become

$$\sigma_{11} = \frac{K_I}{(2\pi r)^{1/2}} \cos \frac{\theta}{2} \left[ 1 - \sin \frac{\theta}{2} \sin \frac{3\theta}{2} \right] \quad (5a)$$

$$\sigma_{22} = \frac{K_I}{(2\pi r)^{1/2}} \cos \frac{\theta}{2} \left[ 1 + \sin \frac{\theta}{2} \sin \frac{3\theta}{2} \right] \quad (5b)$$

$$\sigma_{12} = \frac{K_I}{(2\pi r)^{1/2}} \sin \frac{\theta}{2} \cos \frac{\theta}{2} \cos \frac{3\theta}{2} \quad (5c)$$

$$u_1 = \frac{K_I}{\mu} \left( \frac{r}{2\pi} \right)^{1/2} \cos \frac{\theta}{2} \left[ 1 - 2\nu + \sin^2 \frac{\theta}{2} \right] \quad (5d)$$

$$u_2 = \frac{K_I}{\mu} \left( \frac{r}{2\pi} \right)^{1/2} \sin \frac{\theta}{2} \left[ 2 - 2\nu + \cos^2 \frac{\theta}{2} \right]. \quad (5e)$$

The stress intensity factor elegantly characterizes a crack, similar to energy release rate G. Equations (5a–e) need to be modified for bodies which are of finite dimensions or where the crack tip is close to one of the free edges of the component. Closed form expression for stress intensity factor is available only for simple cases and, therefore, determining the stress intensity factor becomes a challenge for many practical cases. These days, numerical techniques are widely used for this very purpose. However, for a body with a crack and known boundary conditions, once the stress intensity factor is determined, the crack is characterized for a designer and then, he can predict whether a crack in the work-component is likely to grow or not.

Stress and displacement equations for the center-cracked body are similar for other modes. For Mode II in plane strain and far field stress  $\sigma_{12} = \tau$  (Fig. 3.3) with  $K_{II} = \tau\sqrt{\pi a}$ ,

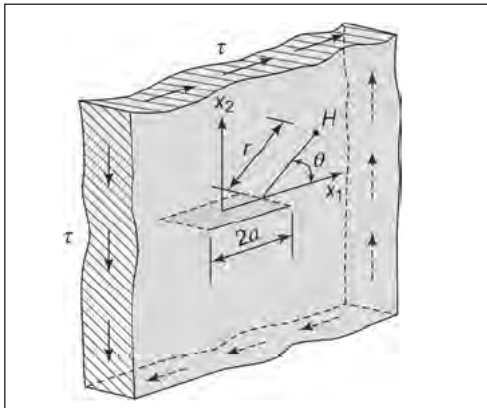


**Fig. 2:** A Center-Crack in An Infinite Plate Loaded in Mode II

we have

$$\sigma_{11} = -\frac{K_{II}}{(2\pi r)^{1/2}} \sin \frac{\theta}{2} \left[ 2 + \cos \frac{\theta}{2} \cos \frac{3\theta}{2} \right] \quad (6a)$$

$$\sigma_{22} = \frac{K_{II}}{(2\pi r)^{1/2}} \sin \frac{\theta}{2} \cos \frac{\theta}{2} \cos \frac{3\theta}{2} \quad (6b)$$

$$\sigma_{12} = \frac{K_{II}}{(2\pi r)^{1/2}} \cos \frac{\theta}{2} \left[ 1 - \sin \frac{\theta}{2} \sin \frac{3\theta}{2} \right] \quad (6c)$$

$$u_1 = \frac{K_{II}}{\mu} \left( \frac{r}{2\pi} \right)^{1/2} \sin \frac{\theta}{2} \left[ 2 - 2\nu + \cos^2 \frac{\theta}{2} \right] \quad (6d)$$

$$u_2 = \frac{K_{III}}{\mu} \left( \frac{r}{2\pi} \right)^{1/2} \cos \frac{\theta}{2} \left[ -1 + 2\nu + \sin^2 \frac{\theta}{2} \right] \quad (6e)$$

$$u_3 = 0. \quad (6f)$$

For Mode III and far field stress  $\sigma_{23} = \tau$  (Fig. 3.4) with  $K_{III} = \tau\sqrt{\pi a}$ , we have

$$\sigma_{11} = \sigma_{22} = \sigma_{33} = \sigma_{12} = 0 \quad (7a)$$

$$\sigma_{13} = -\frac{K_{III}}{(2\pi r)^{1/2}} \sin \frac{\theta}{2} \quad (7b)$$

$$\sigma_{23} = \frac{K_{III}}{(2\pi r)^{1/2}} \cos \frac{\theta}{2} \quad (7c)$$

$$u_1 = u_2 = 0 \quad (7d)$$

$$u_3 = \frac{K_{III}}{\mu} \left( \frac{2r}{\pi} \right)^{1/2} \sin \frac{\theta}{2} \quad (7e)$$

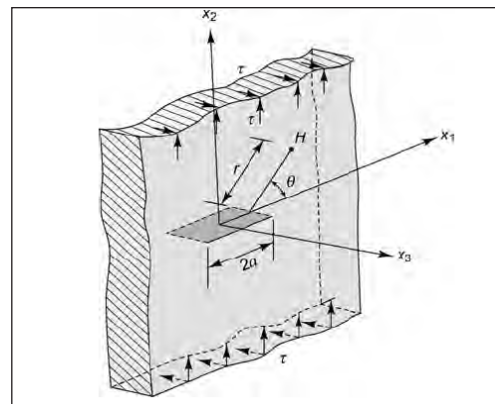


**Fig 3:** A Center-Crack in an Infinite Plate Loaded in Mode III

### MATHEMATICAL MODEL FOR SEMI ELLIPTICAL CRACK

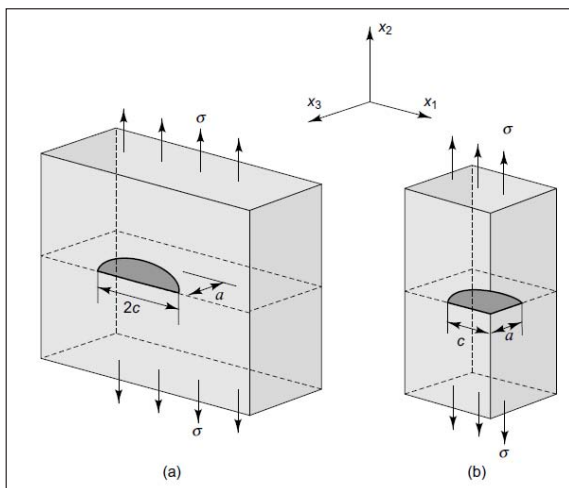
So far we have considered through-the-thickness cracks, i.e., the crack front runs from one face of the plate to another. But there are many cracks of practical importance where a crack initiates at one face of the plate, but does not go all the way to the other face. The front of such a crack is usually curved and embedded within the thickness of the

plate. Embedded cracks are usually modeled as a semi-ellipse in the literature of fracture mechanics. Figure 4(a) shows an embedded crack, also known as surface crack. If the crack happens to be at the corner of the plate (Fig. 4(b)), it is usually modeled as a quarter-elliptical-crack.

When a semi-elliptical crack becomes critical, it may grow along the minor axis  $a$ , or major axis  $c$ , or along both. Later in this section, we would show that for  $c > a$ , the crack in most cases tends to grow more into the depth and less along the lateral direction.

Surface cracks are observed in boilers, compressor-chambers, pipelines, etc., which carry high pressure fluids or gases. Also, many structural components with embedded cracks are subjected to flexural loads. The SIF of some important cases may be obtained from handbooks mentioned in references [3, 4] or other resources mentioned in references [5, 6, and 7]. The SIF may also be determined using a FEM computer package.

It is worth noting that embedded cracks, such as those shown in Fig. 4a are exposed to a free surface of the plate. The free surface influences the stress field and the SIF considerably. Therefore, the analysis of an embedded crack, with its crack face meeting the surface of the plate, is complex and one generally determines SIF through numerical techniques. However, one way to estimate the SIF of surface cracks is by considering the solution to an elliptical crack that is fully embedded in a plate, as shown in Fig. 5. Once the solution to this problem is obtained, the SIF of the semi-elliptical crack is approximated to be 12% higher, similar to the practice adopted for through-the-thickness edge cracks.



**Fig. 4:** (a): A Semi-Elliptical Surface Crack, and (b): A Quarter-Elliptical Corner Crack

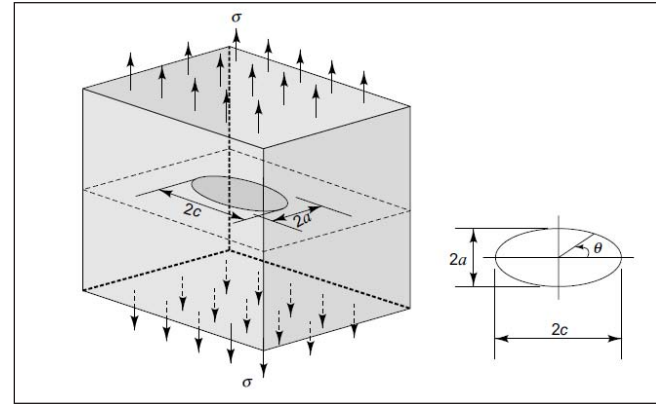


**Fig. 5:** A Fully Embedded Elliptical Crack

As mentioned before, a surface crack is modeled as a half ellipse with its minor axis into the thickness direction. The SIF of the surface crack is then 12% higher over the corresponding SIF of the elliptical crack. Thus, the SIF at a point of the crack front of a semi-elliptical crack is

$$K_I = \frac{1.12\sigma(\pi a)^{1/2}}{I_2} \left[ \sin^2 \theta + \left(\frac{a}{c}\right)^2 \cos^2 \theta \right]^{1/4} \quad (8)$$

At the extreme end of the minor axis ( $\theta = 90^\circ$ ), the SIF is

$$K_I^{90} = \frac{1.12\sigma(\pi a)^{1/2}}{I_2} \quad (9)$$

and at the extreme end of the major axis of the ellipse ( $\theta = 0^\circ$ ), the SIF is given by

$$K_I^0 = \frac{1.12\sigma(\pi a)^{1/2}}{I_2} \left(\frac{a}{c}\right)^{1/2} \quad (10)$$

It is worth noting that the segment of the crack tip, which is deep inside the material, possesses a higher SIF. Thus, a crack tends to grow deeper into the thickness, rather than sideways on the surface, as shown in Fig. 6.

Also, for a very shallow crack ( $a \ll c$ ),  $I_2$  is close to unity as per the equation 11

$$I_2 = \int_0^{\pi/2} \left( 1 - \frac{c^2 - a^2}{c^2} \sin^2 \alpha \right)^{1/2} d\alpha \quad (11)$$

and the SIF at  $\theta = 90^\circ$ , becomes

$$K_I^{90} = 1.12\sigma(\pi a)^{1/2} \quad (12)$$

which is the same as the result of through-the-thickness edge crack of length  $a$ . In this case, the dimension of the

major axis is no longer relevant. Therefore, a shallow crack is equivalent to a through-the-thickness edge crack of length  $a$ .

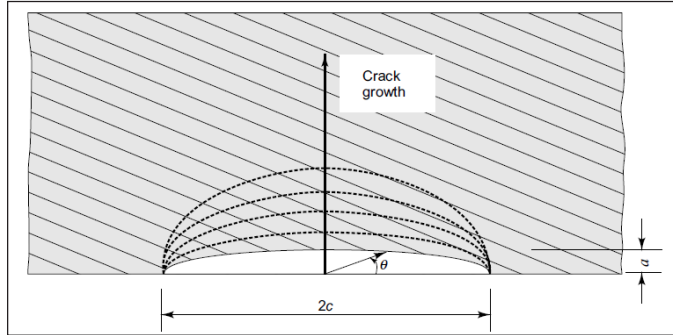


**Fig 6: The Growth of A Semi-Elliptical Surface-Crack**

The problem of the surface crack in a plate, where the crack depth  $a$  is comparable to thickness of the plate, has also been solved through finite element methods [4]. The SIF at the deepest segment of the crack front is expressed as

$$K_I = M\sigma \frac{(\pi a)^{1/2}}{I_2} \quad (13)$$

where the factor  $M$  is 1.12 for a very small  $a/t$ ,  $t$  being the plate thickness.  $M$  increases with the increasing  $a/t$ , but it depends on two ratios,  $a/t$  and  $a/c$ . For further details, readers are referred to a handbook on stress intensity factors [4].

### NUMERICAL VALIDATION OF A SEMI ELLIPTICAL CRACK

Here in this work a semi elliptical crack has been modeled in a block of following dimension 50mm x 50mm x 20mm and the semi elliptical crack has the dimension of 5 mm major axis, 4 mm minor axis and 1mm contour radius with 16 contours.

Now above model with centralized semi elliptical crack model has been subjected to a tensile pressure load of 100 MPa on one transverse surface and other transverse surface has been fixed.

Now for this loading and Boundary conditions stress concentration will be generated and Stress Concentration factors ( $K_1$ ,  $K_2$  and  $K_3$ ) can be calculated through the evaluation of J-Integral as follows

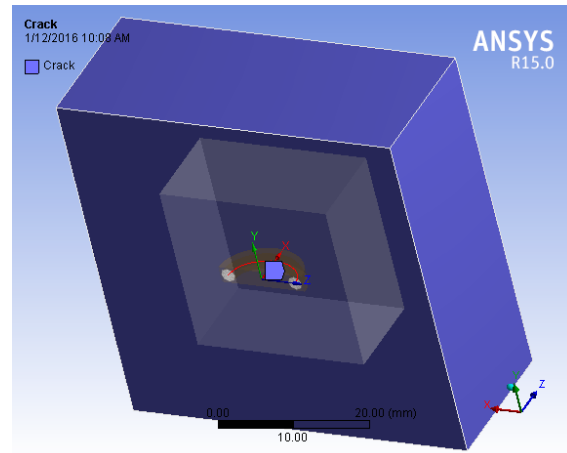


**Fig. 7: A Square Block with Semi-Elliptical Crack**

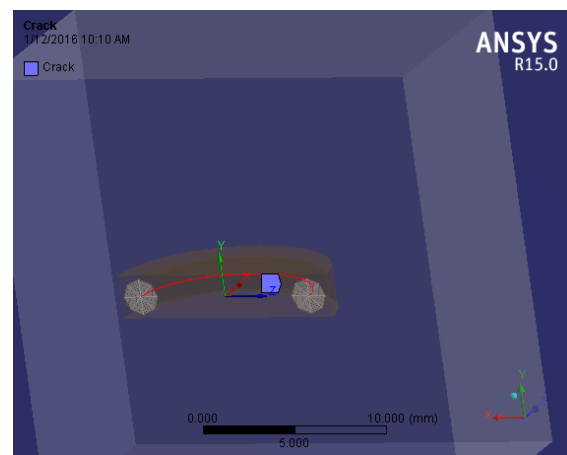


**Fig. 8: Detailed View of Crack**

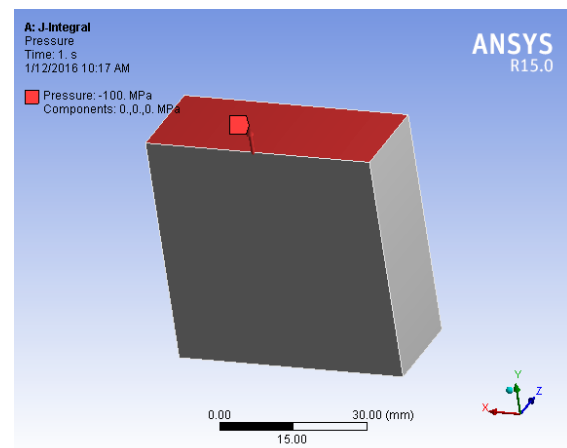


**Fig. 9: Imposed Pr. Load**

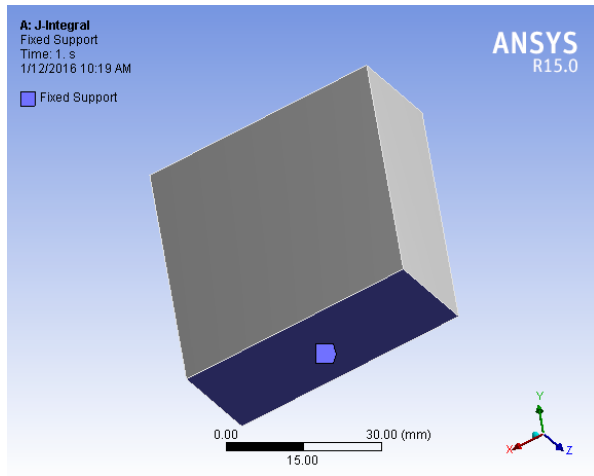


**Fig. 10: Imposed Fixed Support**

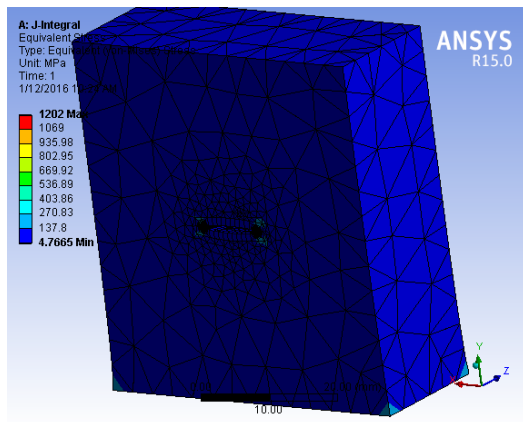


**Fig. 11: Von Misses Stress Distribution Over Whole Object**

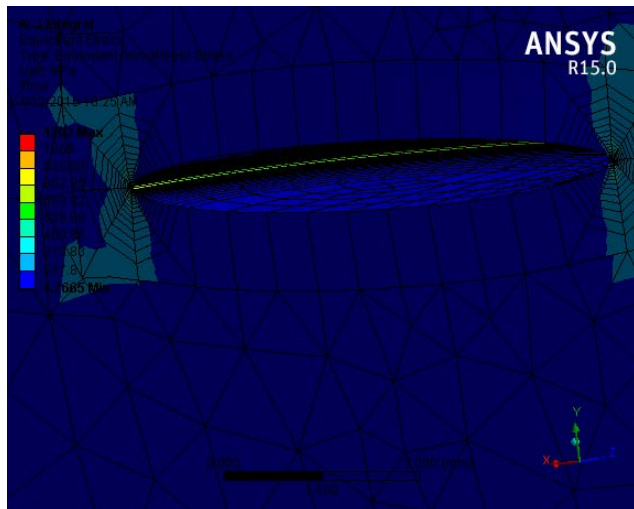
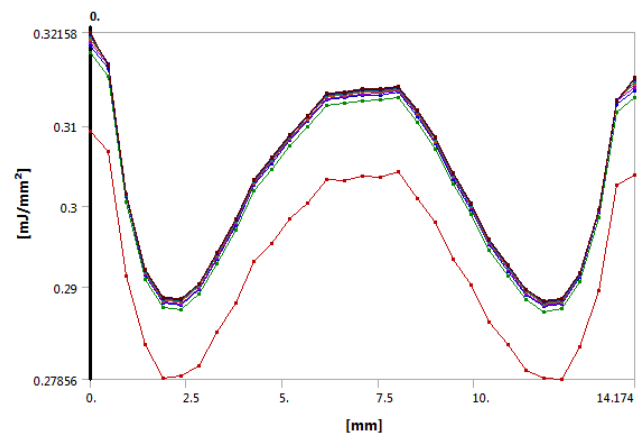


**Fig. 12: Von Misses Stress Distribution Around Crack Showing Stress Concentration**

Now Stress Concentration Factors for three mode of cracks have been tabulated below

Length [mm]	SIFS (K1) Contour 1 [MPa-mm <sup>0.5</sup> ]	SIFS (K1) Contour 2 [MPa-mm <sup>0.5</sup> ]	SIFS (K1) Contour 3 [MPa-mm <sup>0.5</sup> ]
0.	160.86	0.29398	-0.14333
0.4723	199.	0.30044	-0.2409
0.94455	155.81	0.10231	-0.24928
1.4169	192.62	-0.14317	-0.23248
1.8892	154.34	-0.23666	-5.0784e-002
2.3617	193.9	-0.23117	6.5122e-004
2.8341	157.46	-1.8237e-002	1.1609e-002
3.3066	198.91	0.26361	-5.7854e-003
3.7791	162.57	0.3899	-0.10324
4.2516	205.22	0.47484	-0.29562
4.7241	167.33	0.14882	-0.27535
5.1967	209.81	-0.21031	-0.26183
5.6693	170.73	-0.39462	-0.13474
6.1418	213.62	-0.57565	-7.9254e-002
6.6144	172.61	-0.38864	3.2641e-002
7.087	214.51	-0.32447	0.10348
7.5596	172.72	-0.20321	1.9029e-002
8.0321	213.94	-0.30163	-0.11045
8.5047	170.96	-0.34651	-0.13287
8.9773	209.68	-0.56202	-0.12209
9.4499	166.76	-0.5755	-5.852e-002
9.9224	204.17	-0.91203	-5.7597e-002
10.395	161.85	-0.90155	9.0151e-003
10.867	198.41	-1.147	0.19356
11.34	157.3	-0.74015	0.31272
11.812	193.83	-0.51834	0.53432
12.285	154.34	-6.2654e-002	0.47761
12.757	192.52	0.29049	0.52344
13.229	155.41	0.42659	0.25053
13.702	197.62	0.66256	0.1509
14.174	159.23	0.58098	7.6664e-002

Figure below shows the variation of J- Integral



## CONCLUSIONS

It can very easily be proved that SIFs of the above mentioned crack model calculated from the analytical formulas are very much in accordance with the numerical results shown above table.

## REFERENCES

- Irwin, G. R. (1958). *Fracture, Handbuch der Physik, S. Flugge* (ed.), Springer-Verlag, Berlin, Vol. VI, pp. 551-590.
- Kanninen, M. F., & Popelar, C. H. (1985). *Advanced Fracture Mechanics*, Oxford University Press, New York.
- Paris, P. C., & Sih, G. C. (1970). *Stress analysis of cracks*, ASTM STP 381, 30-83.
- Murakami, Y. (1987). *Stress intensity factors handbook*. Pergamon Press, Oxford.
- Broek, D. (1982). *Elementary engineering fracture mechanics*. Martinus Nijhoff Publishers, The Hague.
- Gdoutos, E. E. (2005). *Fracture mechanics-An introduction*. Springer, -The Netherland
- Hellan, K. (1985). *Introduction to fracture mechanics*. McGraw-Hill Book Company, New York.
- Chul-Goo, K., Kyung-Dong, B., Yun-Jae, K., Young-Jin, O., & Budden, P. J. (2015). Reference stress based J & COD estimation of circumferential through-wall cracked elbows under in-plane bending. *Engineering Fracture Mechanics*, 142, 303-317.
- Judt, P. O., & Ricoeur, A. (2015). Crack growth simulation of multiple cracks systems applying remote contour interaction integrals. *Theoretical and Applied Fracture Mechanics*, 75, 78-88.
- Seifi, R. (2015). Stress intensity factors for internal surface cracks in autofrettaged functionally graded thick cylinders using weight function method. *Theoretical and Applied Fracture Mechanics*, 75, 113-123.
- Xie, Y. J., Li, J., Hu, X. Z., Wang, X. H., Cai, M., & Wang, W. (2013). Modelling of multiple crack-branching from Mode-I crack-tip in isotropic solids. *Engineering Fracture Mechanics*, 109, 105-116